Acta Crystallographica Section F
Structural Biology and Crystallization Communications
ISSN 1744-3091

Purification, crystallization and preliminary X-ray characterization of *Bacillus cereus* arylamine *N*-acetyltransferase 3 [(BACCR)NAT3]

Xavier Kubiak,[a] Benjamin Pluvinage,[a]‡ Inès Li de la Sierra-Gallay,[b] Patrick Weber,[c] Ahmed Haouz,[c] Jean-Marie Dupret[a] and Fernando Rodrigues-Lima[a]*

[a]Université Paris Diderot, Sorbonne Paris Cité, Unité de Biologie Fonctionnelle et Adaptative, CNRS EAC 4413, 75013 Paris, France, [b]Université Paris-Sud, Institut de Biochimie et Biophysique Moléculaire et Cellulaire, CNRS UMR 8619, 91405 Orsay, France, and [c]Institut Pasteur, Plateforme 6, CNRS URA 2185, 25 Rue du Dr Roux, 75724 Paris, France

‡ Current address: Biochemistry and Microbiology, University of Victoria, Victoria, British Columbia, Canada.

Correspondence e-mail: fernando.rodrigues-lima@univ-paris-diderot.fr

Received 15 November 2011
Accepted 14 December 2011

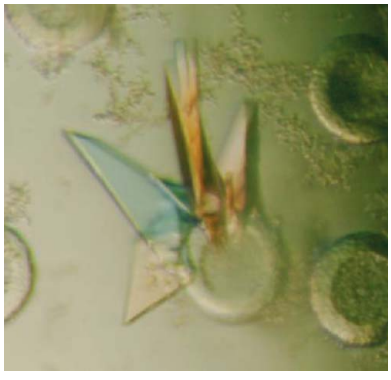

Arylamine *N*-acetyltransferases (NATs) are xenobiotic metabolizing enzymes (XMEs) that catalyze the acetylation of arylamines. All functional NATs described to date possess a strictly conserved Cys-His-Asp catalytic triad. Here, the purification, crystallization and preliminary X-ray characterization of *Bacillus cereus* arylamine *N*-acetyltransferase 3 [(BACCR)NAT3], a putative NAT isoenzyme that possesses a unique catalytic triad containing a glutamate residue, is reported. The crystal diffracted to 2.42 Å resolution and belonged to the monoclinic space group *C*121, with unit-cell parameters $a = 90.44$, $b = 44.52$, $c = 132.98$ Å, $\beta = 103.8^{\circ}$.

1. Introduction

Arylamine *N*-acetyltransferases are phase II xenobiotic metabolizing enzymes that catalyze the transfer of an acetyl group from acetyl-coenzyme A (AcCoA) to a large class of aromatic amine compounds, including drugs, industrial compounds and carcinogens (Riddle & Jencks, 1971; Hein *et al.*, 2000; Dupret & Rodrigues-Lima, 2005). These enzymes are present in several prokaryotic and eukaryotic species (Rodrigues-Lima & Dupret, 2002; Sim, Lack *et al.*, 2008). The crystal structures of several NAT enzymes and mutational studies have underlined the importance of the cysteine-protease-like catalytic triad (Cys-His-Asp; Sim, Walters *et al.*, 2008; Sinclair *et al.*, 2000). Substitution of the Cys or His residues of the triad leads to a complete loss of enzyme activity (Sandy *et al.*, 2005). Recently, studies of a human NAT2 single-nucleotide polymorphism (NAT2*12D) have shown that substitution of the catalytic triad residue Asp122 can have a dramatic impact on the activity of the enzyme (Zang *et al.*, 2007). Surprisingly, mutation of Asp122 to Glu122 resulted in an enzyme with very low activity (more than 40-fold less active than the reference enzyme; Zang *et al.*, 2007). Although the Asp residue is highly conserved and is present in the majority of NAT sequences, certain NAT orthologues from *Bacillus* species have been shown to possess a Glu residue instead of the canonical Asp in their catalytic triad (Sandy *et al.*, 2005; Pluvinage *et al.*, 2007). In *B. cereus*, one of the three NAT isoenzymes, (BACCR)NAT3, has a Glu residue in its catalytic triad (Glenn *et al.*, 2011) but nonetheless appears to be as active as other known NAT enzymes towards several prototypic NAT substrates (unpublished results). (BACCR)NAT3 shares between 25 and 44% amino-acid sequence identity with other characterized bacterial NAT enzymes and possesses the characteristic conserved NAT functional motifs (Rodrigues-Lima & Dupret, 2002; Sandy *et al.*, 2005). This supports the theory that (BACCR)NAT3 is likely to have the same overall fold as other NAT enzymes.

In order to better understand the topology of the Cys-His-Glu catalytic triad in the active site of (BACCR)NAT3, we have undertaken structural studies of this NAT enzyme. Here, we report the expression, purification, crystallization and preliminary X-ray diffraction results of the (BACCR)NAT3 protein.

2. Materials and methods

2.1. Cloning

The *nat* open reading frame coding for the (BACCR)NAT3 protein (GenBank code NP_833217.1) was amplified by polymerase chain reaction (PCR) using the following primers: 5′-CCGGATCCATGACCGACTTTCAAAAACA-3′ [(BACCR)NAT3 forward primer] and 5′-GGGAGCTCTTATAATGTAATTCCGTT-3′ [(BACCR)NAT3 reverse primer]. DNA extracted from *B. cereus* strain ATCC 14597 (kindly provided by Professor I. Martin-Verstraete, Pasteur Institute, Paris) was used as template. The PCR reaction consisted of 40 cycles of denaturation at 367 K (1 min), hybridization at 325 K (30 s) and extension at 345 K (2 min). PCR products were double-digested using *Bam*HI and *Xho*I restriction enzymes (New England Biolabs) and subcloned into pET28a plasmid. Cloning was verified by DNA sequencing.

2.2. Expression and purification

The expression and purification of recombinant (BACCR)NAT3 as an N-terminally 6×His-tagged protein was conducted using a standard procedure described by Pluvinage *et al.* (2007). To remove the 6×His tag, the protein was incubated for 1.5 h with 0.25 µg thrombin (3143.6 NIH units per milligram; Sigma) per milligram of recombinant protein at room temperature. The digested protein was further purified by ion-exchange chromatography (Mono Q, GE Healthcare). The protein was concentrated to 30 mg ml^{-1} using Spin-X UF ultracentrifugation concentrators (10 kDa molecular-weight cutoff, Corning) and kept at 277 K until use. Purity and thrombin digestion of the protein samples were verified by SDS–PAGE and Western blotting using antibodies raised against 6×His tag (Euromedex). The protein concentration was determined from the absorbance at 280 nm.

2.3. Crystallization

Initial identification of crystallization conditions was carried out by the vapour-diffusion method using a Cartesian Technologies workstation (Santarsiero *et al.*, 2002). Sitting drops were set up using 600 nl of a 1:1 mixture of (BACCR)NAT3 protein and crystallization solution (672 different commercially available conditions) and equilibrated against 150 µl reservoir in a Greiner plate (Greiner Bio-One). Optimization of initial hits was pursued manually in Linbro plates with a hanging-drop setup. The best crystals were obtained by mixing 1.5 µl native (BACCR)NAT3 protein at 30 mg ml^{-1} with 1.5 µl reservoir solution consisting of 1.37 *M* sodium citrate pH 6.5 with 0.28 *M* of the additive NDSB-221 (Hampton Research) at 291 K. The crystals appeared within 3–4 weeks and had dimensions of up to 0.1 × 0.1 × 0.05 mm. Single crystals of (BACCR)NAT3 protein were flash-cooled in liquid nitrogen using a mixture of 50% Paratone-N and 50% paraffin oil as cryoprotectant.

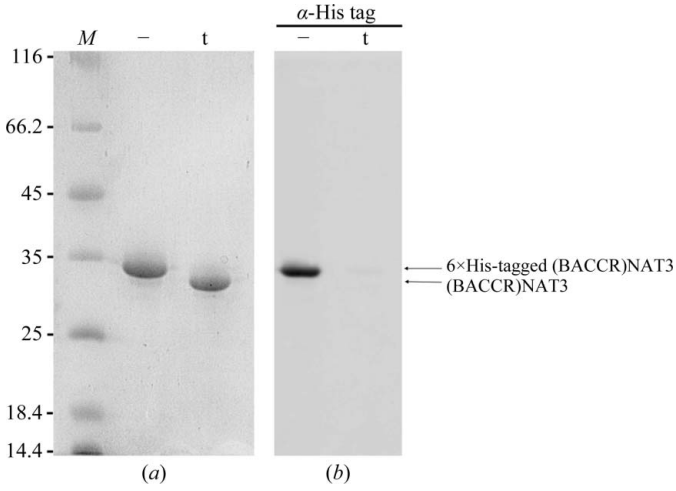

Figure 1
Purification of (BACCR)NAT3 and control of 6×His-tag removal by thrombin digestion. (*a*) The purity level of the recombinant protein was assessed by SDS–PAGE under reducing conditions. 4 µg tagged (−) or thrombin-digested (t) protein was loaded and stained with Coomassie Blue. (*b*) Cleavage of the 6×His tag by thrombin was checked by Western blot analysis. 1 µg native (−) or digested (t) enzyme was separated on SDS–PAGE and Western blotting was achieved using a monoclonal antibody raised against 6×His tag (1:5000 dilution).

2.4. Data collection

Diffraction data were collected at 100 K on beamline PX3 at the Swiss Light Source (Paul Scherrer Institute, Switzerland) using a MAR225 CCD detector with 1 s exposure time. 360 images were collected with 1° oscillation per image at a wavelength of 0.984 Å. The images were integrated with the program *XDS* (Kabsch, 2010) and processed using the *CCP*4 program suite (Winn *et al.*, 2011).

3. Results and discussion

(BACCR)NAT3 has been reported to possess a glutamate residue in its catalytic triad instead of an aspartate (Sandy *et al.*, 2005). Although it has been shown that such a substitution is deleterious to the activity of human NAT2, (BACCR)NAT3 shows N-acetylation activity towards prototypic NAT substrates (such as 4-aminosalicylate, isoniazid and 2-aminofluorene) similar to those reported for well known NATs (unpublished work). Furthermore, the substitution of the catalytic triad aspartate residue by glutamate has also been linked to a strong decrease in protein stability, leading to its rapid degradation (Zang *et al.*, 2007). However, as shown in Fig. 1, (BACCR)NAT3 was easily purified to homogeneity. The major protein band observed at 33 kDa was consistent with the predicted protein molecular mass. No particular proteolysis was observed and the recombinant protein was readily detected by an antibody raised against the 6×His tag (Fig. 1). This tag was efficiently removed by thrombin cleavage, as shown in Fig. 1(*b*). Two extra residues (glycine–serine) from the cloning remain at the N-terminus of the crystallized protein.

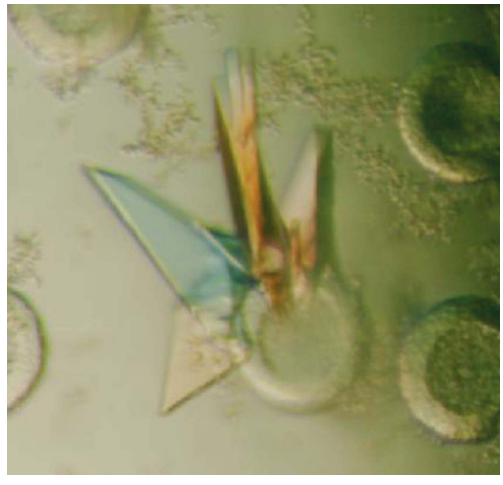

Figure 2
Crystals of (BACCR)NAT3 grown by the hanging-drop vapour-diffusion method in 1.37 *M* sodium citrate pH 6.5, 0.28 *M* NDSB-221 at 291 K. Crystal dimensions are approximately 100 × 100 × 50 µm.

Table 1
Data-collection statistics for the (BACCR)NAT3 crystal.

Values in parentheses are for the highest resolution shell.

X-ray source	Beamline PX3, Swiss Light Source
Wavelength (Å)	0.984
Temperature (K)	100
Unit-cell parameters (Å, °)	a = 90.44, b = 44.52, c = 132.98, $\alpha = \gamma$ = 90.0, β = 103.8
Space group	$C121$
Resolution limits (Å)	20.0–2.425
No. of observations	147178 (22195)
No. of unique reflections	19910 (3060)
$R_{\rm merge}$† (%)	11.3 (43.7)
Completeness (%)	99.3 (97.2)
$\langle I/\sigma(I)\rangle$	19.07 (4.28)

† $R_{\rm merge} = \sum_{hkl}\sum_i |I_i(hkl) - \langle I(hkl)\rangle| / \sum_{hkl}\sum_i I_i(hkl)$, where $I_i(hkl)$ is the ith observation of reflection hkl and $\langle I(hkl)\rangle$ is the mean intensity of reflection hkl.

Crystallization trials were carried out using a wide variety of screening kits. Initial crystallization conditions (1.6 *M* sodium citrate pH 6.5) were significantly optimized by the use of Additive Screen HT (Hampton Research). In particular, NDSB-201, NDSB-211 and NDSB-221 (0.28 *M*) significantly increased crystal growth and decreased nucleation. However, varying the protein:precipitant ratio in crystallization trials was not beneficial. Finally, a single optimized condition produced crystals suitable for X-ray diffraction (Fig. 2): 1.37 *M* sodium citrate pH 6.5, 0.28 *M* NDSB-221.

Crystals grew within 3–4 weeks to maximum dimensions of 0.1 × 0.1 × 0.05 mm. A complete X-ray diffraction data set was collected to 2.42 Å resolution. Data-collection statistics are presented in Table 1. The crystal had monoclinic symmetry, with unit-cell parameters a = 90.44, b = 44.52, c = 132.98 Å, $\alpha = \gamma$ = 90.0, β = 103.8°, and belonged to space group $C121$. Molecular-replacement calculations were carried out with the program *Phaser* (McCoy *et al.*, 2007) as implemented in the *CCP*4 package. The molecular-replacement search model was based on the atomic coordinates of (BACAN)NAT1 (PDB entry 3lnb), recently solved in our laboratory (Pluvinage *et al.*, 2011), which has 44% sequence identity to (BACCR)NAT3. A clear solution was obtained in $C121$ for two independent molecules forming a dimer in the asymmetric unit. The translational Z-score values (TFZ; McCoy *et al.*, 2007) were 15.2 and 44.1, with increasing log-likelihood gain (LLG; McCoy *et al.*, 2007) values of 436 and 2168, respectively. The corresponding highest translational Z-score value was 35.1 and no positive LLG values were obtained for more than a single molecule. This solution corresponds to a solvent content ($V_{\rm s}$) of 46.02% with a Matthews coefficient ($V_{\rm M}$) of 2.28 Å^3 Da^{-1} (Kantardjieff & Rupp, 2003). A model of the (BACCR)NAT3 protein is currently being built and refined. The structure should provide a better understanding of the topology of the unusual catalytic triad of this NAT isoenzyme.

This work was supported by Université Paris Diderot Paris 7, Délégation Générale de l'Armement and Caisse d'Assurance Maladies des Professions Libérales de Province (CAMPLP).

References

Dupret, J.-M. & Rodrigues-Lima, F. (2005). *Curr. Med. Chem.* **12**, 311–318.
Glenn, A. E., Karagianni, E. P., Ulndreaj, A. & Boukouvala, S. (2011). *FEBS Lett.* **584**, 3158–3164.
Hein, D. W., McQueen, C. A., Grant, D. M., Goodfellow, G. H., Kadlubar, F. F. & Weber, W. W. (2000). *Drug Metab. Dispos.* **28**, 1425–1432.
Kabsch, W. (2010). *Acta Cryst.* D**66**, 125–132.
Kantardjieff, K. A. & Rupp, B. (2003). *Protein Sci.* **12**, 1865–1871.
McCoy, A. J., Grosse-Kunstleve, R. W., Adams, P. D., Winn, M. D., Storoni, L. C. & Read, R. J. (2007). *J. Appl. Cryst.* **40**, 658–674.
Pluvinage, B., Dairou, J., Possot, O. M., Martins, M., Fouet, A., Dupret, J.-M. & Rodrigues-Lima, F. (2007). *Biochemistry*, **46**, 7069–7078.
Pluvinage, B., Li de la Sierra-Gallay, I., Kubiak, X., Xu, X., Dairou, J., Dupret, J.-M. & Rodrigues-Lima, F. (2011). *FEBS Lett.* **585**, 3947–3952.
Riddle, B. & Jencks, W. P. (1971). *J. Biol. Chem.* **246**, 3250–3258.
Rodrigues-Lima, F. & Dupret, J.-M. (2002). *Biochem. Biophys. Res. Commun.* **293**, 783–792.
Sandy, J., Mushtaq, A., Holton, S. J., Schartau, P., Noble, M. E. & Sim, E. (2005). *Biochem. J.* **390**, 115–123.
Santarsiero, B. D., Yegian, D. T., Lee, C. C., Spraggon, G., Gu, J., Scheibe, D., Uber, D. C., Cornell, E. W., Nordmeyer, R. A., Kolbe, W. F., Jin, J., Jones, A. L., Jaklevic, J. M., Schultz, P. G. & Stevens, R. C. (2002). *J. Appl. Cryst.* **35**, 278–281.
Sim, E., Lack, N., Wang, C.-J., Long, H., Westwood, I., Fullam, E. & Kawamura, A. (2008). *Toxicology*, **254**, 170–183.
Sim, E., Walters, K. & Boukouvala, S. (2008). *Drug Metab. Rev.* **40**, 479–510.
Sinclair, J. C., Sandy, J., Delgoda, R., Sim, E. & Noble, M. E. (2000). *Nature Struct. Biol.* **7**, 560–564.
Winn, M. D. *et al.* (2011). *Acta Cryst.* D**67**, 235–242.
Zang, Y., Zhao, S., Doll, M. A., States, J. C. & Hein, D. W. (2007). *Pharmacogenet. Genomics*, **17**, 37–45.